URSI AT-AP-RASC 2022, Gran Canaria, Spain, 29 May - 3 June 2022

End-fire antenna array with metamaterial decoupling structures for UAV-borne radar

Christos Milias*[(1)], Rasmus B. Andersen[(1)], Pavlos I. Lazaridis[(2)], Zaharias D. Zaharis [(3)], Bilal Muhammad [(4)], Jes T. B. Kristensen [(1)], Albena Mihovska [(4)], and Dan D. S. Hermansen [(1)],
(1) MyDefence A/S, Noerresundby 9400, Denmark.
(2) University of Huddersfield, Huddersfield, HD1 3DH, UK.
(3) Aristotle University of Thessaloniki, Thessaloniki, 54124, Greece.
(4) Aarhus University, 7400 Herning, Denmark.

Abstract

This paper presents the design and implementation of an X-band, 2D, end-fire antenna array that is suitable for UAV-borne radar applications. The array is synthesized by eight printed Yagi-Uda individual antennas arranged in a 4 x 2 configuration and has a 17dBi gain. Each antenna is fed by a microstrip balun and consists of one driven dipole, one reflector and six directors. Since mutual coupling is detrimental to the performance of phased arrays, metamaterial decoupling structures are utilized to enhance the isolation between them. More specifically, mu-negative meanders are inserted between the elements in the E-plane, while a metasurface of ring resonators isolates the elements in the H-plane. As a result, the inter-element coupling is lower than -30dB. The proposed platform can be easily mounted on unmanned aerial vehicles (UAVs) and is an ideal candidate for UAV-borne radars. Simulations along with measurements verify the effectiveness of our design.

1 Introduction

As the penetration of UAVs into the global market becomes a reality, several practical challenges emerge [1]. Safe navigation of UAVs is one of the main concerns and there is a variety of possible navigation solutions (e.g. cameras, infrared sensors, radars), each one having its own advantages and disadvantages. Radars are one of the most promising candidates, since they offer all-weather operation, wide coverage and long detection range that can be translated into early warnings. For this reason, they are ideal for sense-and-avoid or other critical civilian and military applications. Unarguably, the integration of a radar platform onto a UAV for detection of other UAVs is not a trivial task. On one hand, radars require high-gain antennas with large physical apertures in order to increase the signal-to-noise ratio (SNR) and detect targets or obstacles that are located far away [2]. This can be detrimental to the UAV's flight performance due to the increased weight and unsuitable aerodynamic profile of these antennas. On the other hand, the higher the gain of the radar's antennas, the less transmitted power is required for the same detection range and thus the UAV can be more power-efficient. Hence, it is obvious that the ideal antennas for a UAV-borne radar should exhibit high gain but also have a reasonable size, aerodynamic profile and low weight [3].

In order to satisfy the aforementioned requirements of a UAV-borne radar, this paper presents the design of an aerodynamic, low-profile, high-gain antenna array. Since inter-element coupling is typically detrimental to the performance of phased arrays, metamaterial structures that suppress the mutual coupling are proposed. The final array offers excellent electromagnetic characteristics and can be easily integrated within a UAV's structure. It is estimated that a UAV-borne radar system equipped with two of these arrays (one transmitting and one receiving) can detect small UAV-targets at a maximum distance of 700 meters while transmitting a power of only a few watts. In addition, the aerodynamic performance of the UAV that carries the radar is not compromised.

2 Element Design

The element of the proposed array is a Yagi-Uda antenna with six directors printed on a 0.508 mm thick Rogers RT5880 substrate that has a dielectric constant $\varepsilon_r = 2.2$. The Yagi-Uda design has been chosen as the array element due to its pure horizontal polarization, high gain and end-fire radiation pattern. The horizontal polarization is required here, since the UAV's horizontal polarization monostatic RCS (Radar Cross Section) is expected to be higher compared to the vertical polarization. To start with, the initial geometric parameters are determined by following some traditional rules-of-thumb in order for the antenna to operate around 10 GHz (X-band) [4]. After this, the antenna is simulated with the help of the CST Microwave Studio in order to fine-tune its parameters through parametric sweeps [5]. Special attention is given to the design of the balun that is necessary for connecting the unbalanced microstrip feed line to the balanced radiating dipole. The operation of the balun relies on the fact that one of its arms introduces an additional 180° phase shift by properly tuning its length to be around $\lambda_g/2$, where λ_g is the guided wavelength of the microstrip line. The final parameters of the Yagi-Uda are determined so that two main conditions are satisfied: i) the antenna resonates at 10 GHz (i.e. return loss higher than 20dB), ii) and the forward realized gain is higher than 9dBi. In addition, the length of the directors is progressively shortened (tapered), in order to reduce the H-plane sidelobes.

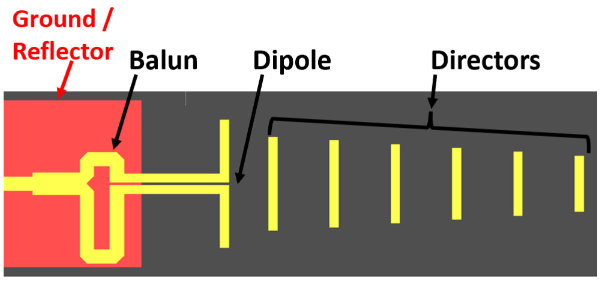

Figure 1

3 Array Design

For the synthesis of the array, the following considerations are taken into account:

- The maximum forward realized gain must be high enough for the successful detection of a target at 700m distance. In order to estimate the required value for the gain, the radar equation is utilized:

$$R_{max} = \sqrt[4]{\frac{P_t G^2 \lambda^2 \sigma}{(4\pi)^3 P_{min}}} \tag{1}$$

  where P_t is the transmitted power which here is assumed to be 10 Watts, G is the realized gain of the radar's antennas (same for transmission and reception), λ is the free-space wavelength (3cm at 10 GHz), σ is the monostatic RCS of a small UAV which is assumed to be 0.02 m^2 and P_{min} is the sensitivity of the receiver (-120 dBm). From the above formula, the required gain is calculated to be 17dBi. Given that a single element offers 9dBi of gain, eight elements have to be combined to reach the specified array gain.

- Radars typically suffer from ground clutter which is detrimental to the sensitivity of the receiver and cause serious performance issues. To mitigate this, the eight Yagi-Uda elements are placed in a 4x2 arrangement so that the elevation beamwidth of the array is reduced compared to the 8x1 arrangement. In this manner, the impact of strong reflections due to the ground underneath the radar can be somewhat alleviated. Of course, this results in an increased azimuth beamwidth.

The next step of the array synthesis is to consider the effects of mutual coupling. Mutual coupling between adjacent elements is detrimental to the performance of phased arrays. As the scan angle varies, the elements become mismatched and most of the power is reflected back to the source. This happens due to the modified input impedance of each individual antenna which is affected by the impedance and phase of its neighbouring elements. In addition, there is a radiation pattern distortion, which can potentially result in lower array gain and higher side lobes. These undesired effects can be suppressed by enhancing the isolation between neighbouring Yagi-Uda elements. Since the proposed array has both vertically and horizontally arranged elements (2D array), the two configurations have to be treated separately. To decouple the horizontally adjacent elements (E-plane), four metamaterial meanders that exhibit negative permeability are inserted between the two dipoles. In a similar manner, a metasurface consisting of ring resonators is placed between the vertically neighbouring elements (H-plane). The meanders and the metasurface prohibit the propagation of electromagnetic waves since they exhibit a stop-band at the desired frequency [6]. As a result, the coupling can be considerably reduced for both configurations. For the design of the metamaterial structures, their unit cell (meander and ring resonator respectively) are simulated and their geometric parameters are tuned so that their transmission response has a null around 10 GHz.

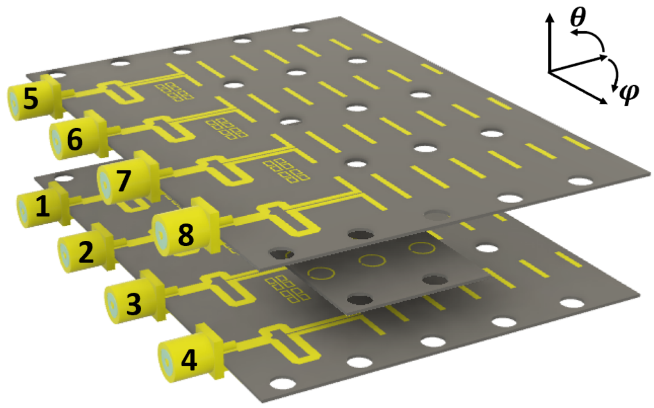

Figure 2. Illustration of the proposed 4x2 array which consists of two 4x1 subarrays in a vertical configuration. The metasurface is placed between the two subarrays.

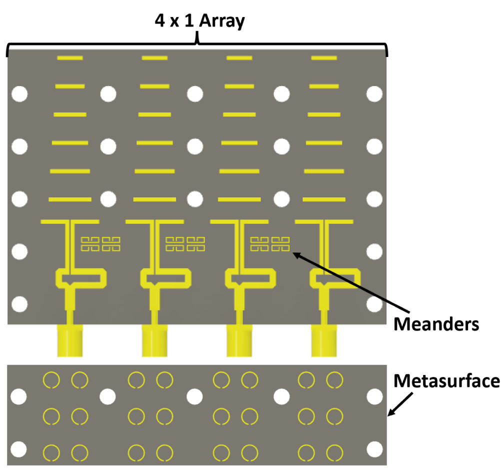

Figure 3. Illustration of the proposed 4x1 array with the metamaterial meanders between the dipoles (top) and the metasurface of ring resonators (bottom).

In order to build the proposed 4x2 array, two 4x1 arrays are combined as shown in Fig. 2. The metamaterial meanders are placed between the horizontally neighbouring dipoles. The metasurface of ring resonators, which is depicted in Fig. 3 and is responsible for the decoupling of the H-plane adjacent elements, is placed between the two 4x1 arrays. Some holes are drilled on the boards of the two 4x1 arrays and metasurface in order to align and connect them together with nylon screws. The final prototype is fabricated and shown in Fig. 4.

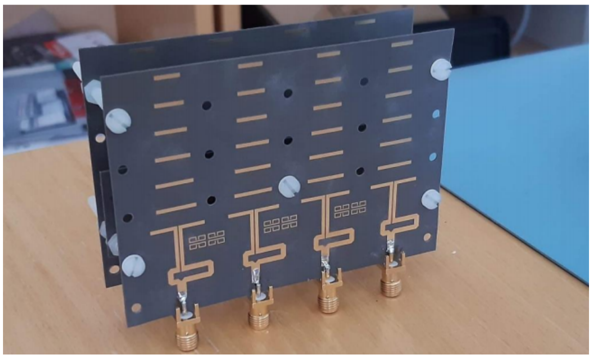

Figure 4. Fabricated prototype of the proposed antenna array.

4 Measurements

The final prototype is fabricated and shown in Fig. 4. The numbering of the Yagis is given in Fig. 2. The measured reflection coefficients S_{ii} $(i = 1,...,8)$ are presented in Fig. 5. As shown, all the elements of the array are well-matched to 50Ω from 9.3 to 10.6 GHz.

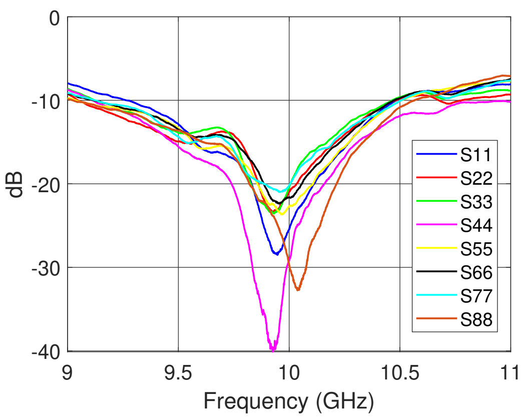

Figure 5. Measured reflection coefficients versus frequency of the eight array elements.

After this, the coupling between horizontally adjacent elements of the array is depicted in Fig. 6. Due to the array's symmetry, only the S_{21} and S_{76} are presented here for demonstration purposes. As shown, the coupling is reduced by almost 15dB when the MTM (metamaterial) meanders are inserted between the dipoles of the Yagi-Udas. Of course, this isolation enhancement is only achieved within the frequency band of interest (i.e. 9.8-10.5 GHz). Similarly, Fig.7 presents the coupling coefficients between vertically neighbouring elements of the array. Here, the S_{51} and S_{71} coefficients are considered as representative examples. As clearly demonstrated, the coupling is reduced by up to 20dB within the desired bandwidth. Hence, the coupling between any two elements of the array is always lower than 25dB (for vertically adjacent elements) and 35dB (horizontally adjacent elemens) within the 9.8-10.5 GHz bandwidth. In parallel, there is a good agreement between the measured and simulated results.

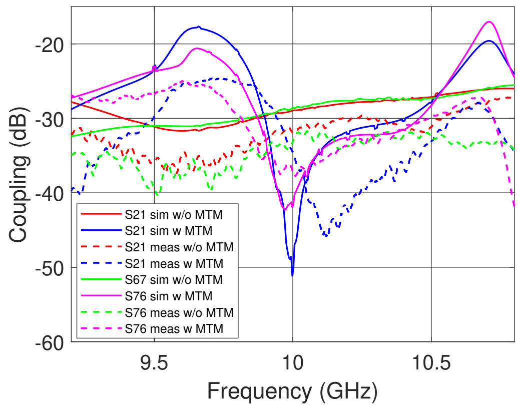

Figure 6. Simulated and measured coupling coefficients S_{21} and S_{76} versus frequency with and without MTM (metamaterials).

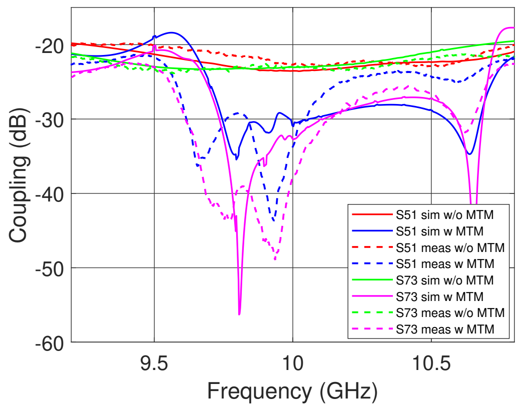

Figure 7. Simulated and measured coupling coefficients S_{51} and S_{73} versus frequency with and without MTM (metamaterials).

The measured and simulated E-plane (azimuth) radiation patterns of the array are given in Fig. 8. The array has a beamwidth of almost 15°, while the simulated and measured sidelobes are -14 and -12.5 dB respectively. Of course, a tapered amplitude distribution can be applied in order to further decrease the sidelobes. Fig. 9 shows the H-plane (elevation) radiation pattern of the array. Here, the beamwidth is almost 30°. In addition, the front-to-back ratio of the array is above 16dB in simulations and 19dB in measurements. Finally, the simulated and measured realized gain of the array with and without the metamaterial structures is provided in Fig. 10. Despite the fact that the gain is reduced at lower frequencies, there is a clear gain enhancement of almost 1dB within the frequency band of interest. This increase is attributed to the lower coupling between the elements.

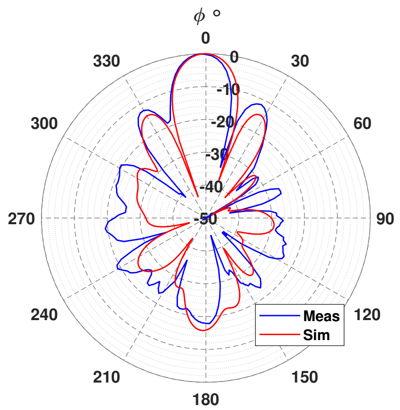

Figure 8. Simulated and measured E-plane (azimuth) radiation pattern of the co-polarization (horizontal) at 10.1 GHz.

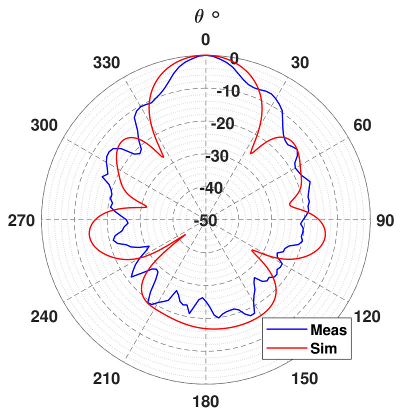

Figure 9. Simulated and measured H-plane (elevation) radiation pattern of the co-polarization (horizontal) at 10.1 GHz.

5 Conclusion

The design and implementation of an aerodynamic antenna array for UAV-borne radar platforms is proposed in this paper. A 9dBi X-band, printed Yagi-Uda antenna is initially designed as the array's element. By taking into account the key aspects of the UAV-borne radar system, a 4x2 array is synthesized and metamaterial structures are designed in order to enhance the isolation between adjacent elements in both planes. The proposed techniques reduce the coupling by at least 15dB from 9.8 to 10.5 GHz without affecting the performance of the array within this frequency band. In particular, the realized forward gain is increased by up to 1dB. Furthermore, the sidelobes and front-to-back ratio of the proposed array are adequate and can be further improved depending on the application requirements. Finally, it is estimated that a UAV-borne radar platform that transmits 10W and is equipped with the proposed array can detect small UAV-targets at a maximum distance of 700m.

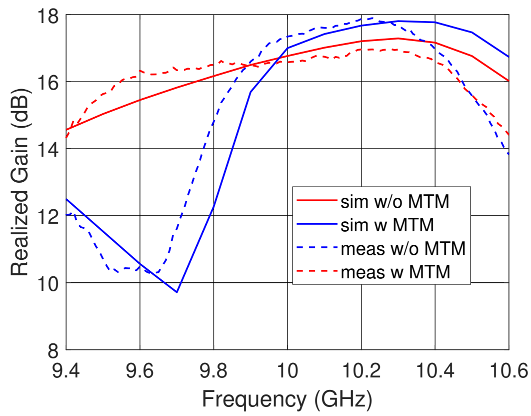

Figure 10. Simulated and measured forward realized gain of the array versus frequency with and without the presence of metamaterial structures.

6 Acknowledgements

This work was supported by the European Union, through the Horizon 2020 Marie Skodowska-Curie Innovative Training Networks Programme "Mobility and Training for beyond 5G Ecosystems (MOTOR5G)" under grant agreement no. 861219.

References

[1] B. Li, Z. Fei, and Y. Zhang, "UAV communications for 5G and beyond: Recent advances and future trends," IEEE Internet Things J., vol. 6, no. 2, pp. 2241–2263, Apr. 2019.

[2] M. I. Skolnik, Introduction to Radar Systems. New York: McGrawHill, 2001

[3] J. J. Peng, S. W. Qu, M. Xia, and S. Yang, "Wide-scanning conformal phased array antenna for UAV radar based on polyimide film," IEEE Antennas Wireless Propag. Lett., vol. 19, no. 9, pp. 1581–1585, Sep. 2020.

[4] C. A. Balanis, "Antenna theory: analysis and design," John wiley and sons, 2016.

[5] CST Microwave Studio. [Online]. Available: http://www.cst.com

[6] C. Milias, R. B. Andersen, P. I Lazaridis, Z. D. Zaharis, B. Muhammad, J. T. B. Kristensen, A. Mihovska and D. D. S. Hermansen, "Metamaterial-inspired Antennas: A Review of the State of the Art and Future Design Challenges," *IEEE Access,* vol. 9, pp. 89846-89865, Jun. 2021.